

# Three-element phased-array approach to diffuse optical imaging based on postprocessing of continuous-wave data

Ning Liu, Angelo Sassaroli, Max A. Zucker, and Sergio Fantini

Department of Biomedical Engineering, Bioengineering Center, Tufts University, 4 Colby Street, Medford, Massachusetts 02155

Received September 1, 2004

We present a multielement phased-array approach to diffuse optical imaging based on postprocessing of continuous-wave data for the improvement of spatial resolution. In particular, we present a theoretical and experimental analysis of the performance of a three-element source array in the study of an optically turbid medium with two embedded cylindrical inclusions. We find that the proposed phased-array approach is able to resolve two cylinders with side-to-side separation of 10 mm that are not resolved by the intensity associated with a single light source. © 2005 Optical Society of America

OCIS codes: 170.0110, 170.5270, 170.6510, 170.6930, 300.1030.

Diffuse optical imaging is a noninvasive technique that finds applications in the study of highly scattering media. One important example is near-infrared imaging of biological tissue in areas such as functional studies of the brain<sup>1</sup> and detection of breast cancer.<sup>2</sup> A limitation of diffuse optical imaging is its relatively low spatial resolution. One of the methods proposed in the literature to better localize optical inclusions is the phased-array method<sup>3–6</sup> that uses two out-of-phase intensity-modulated light sources. The approach described here is an extension of the previous phased-array method in that it uses a three-element (either three sources or three detectors) array to collect continuous-wave (cw) data and a postprocessing scheme of data analysis to introduce specific amplitude–phase relationships among the three elements.

Let us consider an array of  $N$  cw light sources and a single optical detector that collects intensity  $I_i$  from the  $i$ th light source. Our phased-array approach consists of normalizing  $I_i$  and introducing amplitude  $A_i$  and phase  $\alpha_i$  factors to obtain a phased-array intensity ( $I_{P-A}$ ) according to the following equation:

$$I_{P-A} = \sum_{i=1}^N A_i \frac{I_i}{I_{0i}} \cos(\alpha_i), \quad (1)$$

where the intensity normalization is performed by dividing  $I_i$  by background intensity  $I_{0i}$ . In this Letter we present the particular case of a single optical detector and an array of three collinear sources, in which each source is separated by 1 cm from the next and the amplitude–phase factors defined in Eq. (1) are  $A_1 = A_3 = 1$ ,  $A_2 = 2$ ,  $\alpha_1 = \alpha_3 = \pi$ , and  $\alpha_2 = 0$ . The single detector is placed across the middle source ( $i = 2$ ) at a distance of 6 cm, which is representative of the source–detector separations used in optical studies of thick tissues. This particular three-source phased array is illustrated in Fig. 1. As a first comparison between the case of a single source–detector pair and the phased-array approach of Fig. 1, we consider the respective areas of sensitivity in a uniform highly scattering medium characterized by an absorption coefficient  $\mu_{a0}$  and a reduced scattering coefficient  $\mu_{s0}'$ . The background intensity  $I_0$  detected at position  $\mathbf{r}_d$  as a result of illumination at position  $\mathbf{r}_s$  is described

by the solution to the diffusion equation, which in an infinite-medium geometry is given by<sup>7</sup>

$$I_0 = \frac{vP}{4\pi D_0} \frac{\exp[-(v\mu_{a0}/D_0)^{1/2}|\mathbf{r}_d - \mathbf{r}_s|]}{|\mathbf{r}_d - \mathbf{r}_s|}, \quad (2)$$

where  $D_0$  is the background diffusion coefficient defined as  $v/[3(\mu_{a0} + \mu_{s0}')]$ ,  $v$  is the speed of light in the medium, and  $P$  is the source power. We define a sensitivity function as a function of position  $\mathbf{r} = (x, y, z)$  as the change in the parameter of interest (single-source intensity  $I$  or phased-array intensity  $I_{P-A}$ ) caused by a small optical perturbation at  $\mathbf{r}$  relative to the change caused by the same perturbation at  $(x_d, y, z_d)$ , where  $x_d$  and  $z_d$  are the  $x$  and  $z$  coordinates of the detector and the  $y$  axis is perpendicular to the linear source array. The first-order perturbation solution to the diffusion equation yields the following expression for the change in intensity  $\Delta I(\mathbf{r})$  caused by a small absorbing object of volume  $V$  at position  $\mathbf{r}$  (Ref. 8):

$$\Delta I(\mathbf{r}) = - \frac{v^2 \Delta \mu_a P V}{(4\pi D_0)^2} \times \frac{\exp[-(v\mu_{a0}/D_0)^{1/2}(|\mathbf{r} - \mathbf{r}_s| + |\mathbf{r}_d - \mathbf{r}|)]}{|\mathbf{r} - \mathbf{r}_s| |\mathbf{r}_d - \mathbf{r}|}, \quad (3)$$

where  $\Delta \mu_a$  is the absorption contrast associated with the object. The intensity measured in the presence of the absorbing defect at position  $\mathbf{r}$  is given by

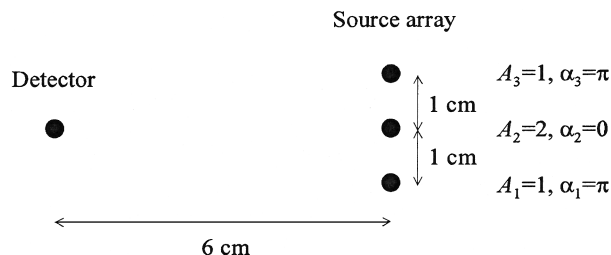


Fig. 1. Representative phased-array consisting of three sources with the indicated amplitude ( $A_i$ ) and phase ( $\alpha_i$ ) factors. These factors are defined in Eq. (1). The detector faces the central source at a distance of 6 cm, and the intersource separation is 1 cm.

$$I(\mathbf{r}) = I_0 + \Delta I(\mathbf{r}). \quad (4)$$

The spatial distribution of the sensitivity function in the plane defined by the detector and by the linear source array of Fig. 1 is shown in Fig. 2 for the intensity due to the central source ( $i = 2$ ) [Fig. 2(a)] and for the phased-array intensity [Fig. 2(b)]. Specifically, the sensitivity functions of Figs. 2(a) and 2(b) are given by  $|\Delta I_2(x, y)/\Delta I_2(0, y)|$  and  $|\Delta I_{P-A}(x, y)/\Delta I_{P-A}(0, y)|$ , where  $\Delta I_{P-A}$  is calculated from the right-hand side of Eq. (1) with  $I_i$  replaced by  $\Delta I_i$  as given by Eq. (3). The region of sensitivity of the phased-array intensity is narrower than that of the single-source intensity, suggesting an improvement in spatial resolution, even though it presents two sidelobes that expand the region of sensitivity toward the source array side.

We performed an experimental test of the improvement in spatial resolution afforded by the proposed three-element phased-array approach. We used three multiplexed (i.e., turned on and off in sequence) laser diodes emitting at 690 nm from a near-infrared tissue spectrometer (OxiplexTS, ISS, Inc., Champaign, Illinois). These laser diodes were coupled to multimode optical fibers, 400  $\mu\text{m}$  in diameter, whose emitting ends were arranged in a linear source array according to the layout in Fig. 1. The collection optical fiber, a fiber bundle with an internal diameter of 3 mm, was also placed according to the geometry in Fig. 1, i.e., facing the central source fiber at a distance of 6 cm. The illumination and collection optical fibers were immersed in a highly scattering liquid sample (2% milk with black India ink added) with an absorption coefficient of  $0.047 \pm 0.002 \text{ cm}^{-1}$  and a reduced scattering coefficient of  $15 \pm 1 \text{ cm}^{-1}$ . At the midplane, i.e., equidistant (3.0 cm) from the source array and the collection fiber, we placed two black cylinders, 0.62 cm in diameter and 12 cm in height. The side-to-side distance between the cylinders was varied from 0 to 9 cm in steps of 0.5 cm. For each cylinder separation we performed a linear tandem scan of the source fiber array and the collection fiber to investigate the level of resolution of the two absorbing cylinders. The linear scanning speed was 0.13 cm/s and the optical sampling rate was 3.125 Hz, so that we acquired one optical data point every 416  $\mu\text{m}$  along the scanning direction. Figure 3 shows the experimental results and theoretical fits for the cases of side-to-side cylinder separations of 70, 20, and 10 mm. In particular, Fig. 3(c) shows the improvement in spatial resolution obtained with the phased-array method. The theoretical fits were performed by use of Eq. (4) for center-source intensity  $I_2$  and Eqs. (1) and (4) for phased-array intensity  $I_{P-A}$ . In this case, Eq. (4) consists of two perturbation terms, one for  $\mathbf{r} = \mathbf{r}_1$  and the other for  $\mathbf{r} = \mathbf{r}_2$  (with  $\mathbf{r}_1$  and  $\mathbf{r}_2$  being the centers of the first and second cylinder, respectively) under the assumption that their contributions combine linearly. The best-fit values of  $V\Delta\mu_a$  for cylinder-to-cylinder separations of 70, 20, and 10 mm, respectively, are  $0.254 \pm 0.002$ ,  $0.249 \pm 0.002$ , and  $0.240 \pm 1 \text{ cm}^2$  for the single-source case and  $0.277 \pm 0.002$ ,  $0.265 \pm 0.002$ , and  $0.344 \pm 0.002 \text{ cm}^2$  for the phased-array case. We also varied the  $(x, y)$  coordinates of the centers of the cylinders to within

their experimental errors, and the theoretical curves in Fig. 3 represent the best match with the experimental data. The good agreement between theory and experiment in Fig. 3 suggests that first-order perturbation theory can be used to predict the shape of the single-source–single-detector and phased-array intensity curves even beyond its small-perturbation limit of quantitative applicability.

Further experimental and theoretical trials confirmed the better performance of the phased array with respect to the one-source–one-detector method. A key result of this study is that the phased-array method shows an asymmetric resolution and contrast performance with respect to the midplane. In fact, the resolution is better close to the single detector [see Fig. 2(b)], whereas the contrast is higher close to the source array. The latter result is due to the fact that the intensities detected from the individual sources become increasingly similar for objects closer to the single detector, and they tend to cancel each other out in the phased-array intensity. The asymmetrical behavior of the phased-array method with respect to the midplane can be exploited to selectively enhance structures located at different depths in the medium.

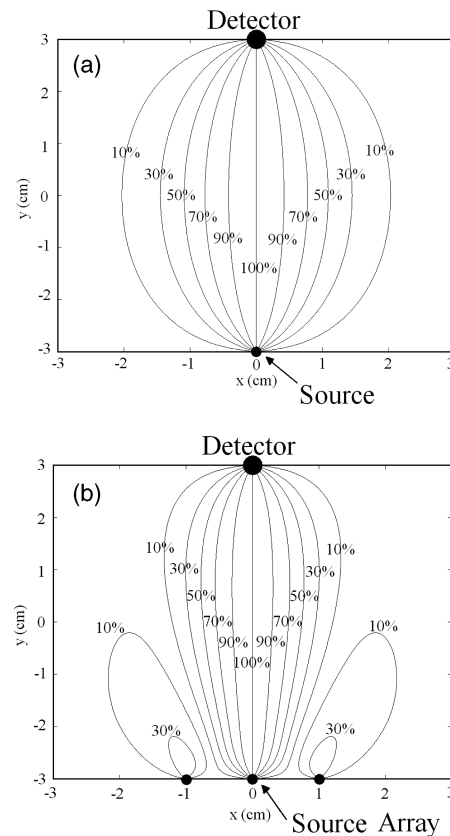


Fig. 2. Spatial distribution of the sensitivity function on the  $x$ - $y$  plane defined by the detector and the source array for (a) one source and one detector located at  $(0, -3)$  and  $(0, 3)$ , respectively, and (b) the three-source array of Fig. 1 consisting of sources located at  $(-1, -3)$ ,  $(0, -3)$ , and  $(1, -3)$ . In both panels, the sensitivity function is defined relative to the value at  $x = 0$  (i.e., along the line through the detector and the central source). The optical coefficients used in Eq. (3) to calculate these sensitivity functions are  $\mu_{a0} = 0.047 \text{ cm}^{-1}$  and  $\mu_{s0}' = 15 \text{ cm}^{-1}$ .

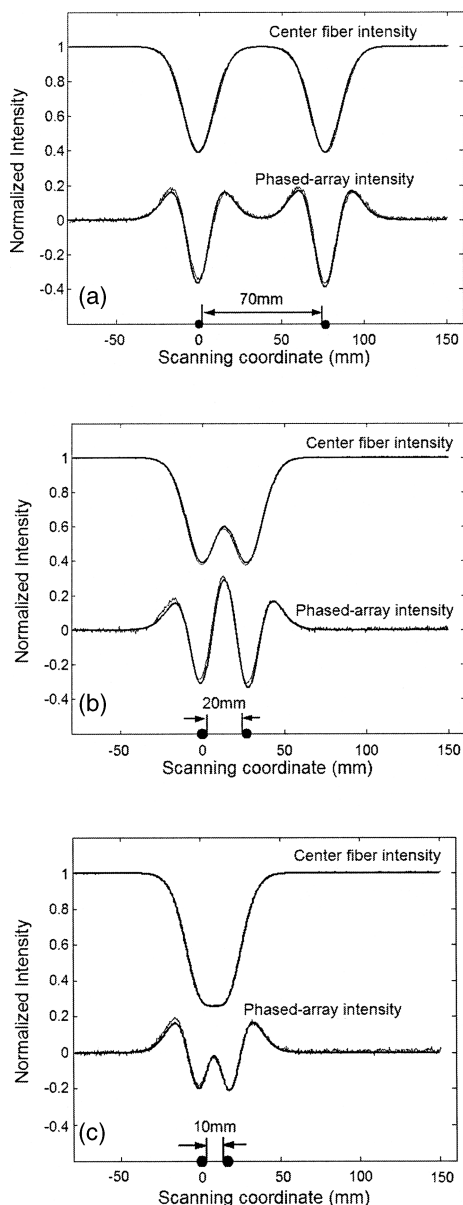


Fig. 3. Experimental results (thin curves) and theoretical fits (thick curves) for center-source intensity  $I_2$  and phased-array intensity  $I_{P.A}$  in the linear scans performed in a highly scattering liquid sample containing two absorbing cylinders located halfway between the source and detector scanning lines. The black dots indicate the positions of the two absorbing cylinders. The side-to-side separation between the cylinders is 70 mm in (a), 20 mm in (b), and 10 mm in (c).

The three-element phased-array method described here is similar to a discrete spatial second derivative of the intensity along the direction of the source array axis. Looking at Fig. 1, one can see that

the three-source phased-array intensity resembles a numerical second derivative of the scanned intensity with a variable step of derivation that is larger close to the source array and smaller close to the detector. We recently showed the effectiveness of the spatial second derivative in enhancing the spatial resolution of optical mammography.<sup>9</sup> The second derivative enhances the minute shape changes of the one-source-one-detector scanned intensity and exploits a unique feature of photon migration not only for edge detection but also for the discrimination of single versus multiple defects.

In summary, we have presented a multielement phased-array approach to diffuse optical imaging that is based on postprocessing of cw data and that has the potential to improve the spatial resolution of optical imaging in highly scattering media. Furthermore the asymmetrical contrast performance of the three-element phased-array method with respect to the midplane can be used to provide depth information. The enhancement in spatial resolution and the capability of depth discrimination render this phased-array method potentially effective in practical applications such as medical imaging.

This work was supported by National Science Foundation award BES-93840 and by National Institutes of Health grants DA14178 and CA095885. N. Liu's e-mail address is ning.liu@tufts.edu.

## References

1. Special Section on Optical Imaging, G. Gratton, M. Fabiani, T. Elbert, and B. Rockstroh, eds., *Psychophysiology* **40**, 487–571 (2003).
2. Special Section on Optics in Breast Cancer, S. Fantini, K. T. Moesta, and B. W. Pogue, eds., *J. Biomed. Opt.* **9**, 1121–1181 (2004).
3. B. Chance, K. Kang, L. He, J. Weng, and E. Sevick, *Proc. Natl. Acad. Sci. USA* **90**, 3423 (1993).
4. K. A. Kang, D. F. Bruley, and B. Chance, *Biomed. Instrum. Technol.* **31**, 373 (1997).
5. J. M. Schmitt, A. Knüttel, and J. R. Knutson, *J. Opt. Soc. Am. A* **9**, 1832 (1992).
6. Y. Chen, C. Mu, X. Intes, and B. Chance, *Appl. Opt.* **41**, 7325 (2002).
7. J. B. Fishkin and E. Gratton, *J. Opt. Soc. Am. A* **10**, 127 (1993).
8. J.-M. Kaltenbach and M. Kaschke, in *Medical Optical Tomography: Functional Imaging and Monitoring*, G. J. Müller, B. Chance, R. R. Alfano, S. R. Arridge, J. Beuthan, E. Gratton, M. Kaschke, B. R. Masters, S. Svanberg, and P. van der Zee, eds. (SPIE Press, Bellingham, Wash., 1993), pp. 65–86.
9. V. E. Pera, E. L. Heffer, H. Siebold, O. Schutz, S. Heywang-Kobrunner, L. Gotz, A. Heinig, and S. Fantini, *J. Biomed. Opt.* **8**, 517 (2003).